THE JOURNAL OF PHYSICAL CHEMISTRY A

Article

Cite This: J. Phys. Chem. A 2018, 122, 5730−5734

pubs.acs.org/JPCA

Carbon Core Electron Spectra of Polycyclic Aromatic Hydrocarbons

Andrew E. Pomerantz,*[,†] Ethan Crace,[‡,§] Tsu-Chien Weng,[§,∥] Dimosthenis Sokaras,[§] and Dennis Nordlund[§]

HPSTAR 600-2018

[†]Schlumberger-Doll Research, Cambridge, Massachusetts 02139, United States

[‡]Department of Chemistry, Stanford University, Stanford, California 94305, United States

[§]SLAC National Accelerator Laboratory, Menlo Park, California 94025, United States

[∥]Center for High Pressure Science & Technology Advanced Research, Shanghai 201203, China

Supporting Information

ABSTRACT: Aromaticity profoundly affects molecular orbitals in polycyclic aromatic hydrocarbons. X-ray core electron spectroscopy has observed that carbon 1s−π^* transitions can be broadened or even split in some polycyclic systems, although the origin of the effect has remained obscure. The π electrons in polycyclic systems are typically classified in the Clar model as belonging to either true aromatic sextets (similar to benzene) or isolated double bonds (similar to olefins). Here, bulk-sensitive carbon core excitation spectra are presented for a series of polycyclic systems and show that the magnitude of the 1s−π^* splitting is determined primarily by the ratio of true aromatic sextets to isolated double bonds. The observed splitting can be rationalized in terms of ground state energetics as described by Hückel, driven by the π electron structure described by Clar. This simple model including only ground state energetics is shown to explain the basics physics behind the spectral evolution for a broad set of polycyclic aromatic hydrocarbons, although some residual deviations between this model and experiment can likely be improved by including a more detailed electronic structure and the core hole effect.

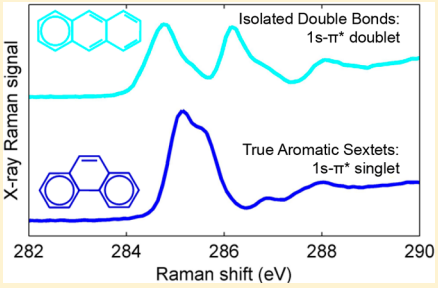

INTRODUCTION

Since its introduction by Kekulé in 1865,[1] the concept of aromaticity has been integral for understanding molecular structure, reactivity, and spectroscopy. Hückel's work provided a criterion for aromaticity and an estimate of the shapes and energies of molecular orbitals (MOs) in monocyclic hydrocarbons,[2−4] and Clar's model extended the concept to polycyclic aromatic hydrocarbons (PAHs).[5] Aromaticity is widely invoked to explain myriad spectral features such as band gaps probed by optical spectroscopy, chemical shifts probed by NMR spectroscopy, and core electron transitions probed by X-ray spectroscopy.[5,6]

In core electron spectroscopy, it has been observed that the line width of the carbon 1s−π^* transition varies for PAHs of different structure, and this spectral feature has been used to assign average molecular geometries in complex mixtures such as petroleum.[6] However, a direct link between the ground state and the 1s−π^* line width variation has not been well-defined, partly because of the complications that arise when a full account of the energetics involved in the X-ray absorption process is taken into account.[7] Here we present carbon K-edge spectra of several PAHs obtained by high-resolution hard X-ray Raman scattering (XRS), taking advantage of the long penetration depth of hard X-rays to provide bulk-sensitive carbon core excitations without experimental artifacts such as surface contamination and normalization difficulties in soft X-ray measurements. We observe that the 1s−π^* line broadening previously observed with a lower-resolution X-ray Raman spectrometer results from a line splitting, which is observable at higher resolution, consistent with other studies on smaller PAH subsets measured with direct soft X-ray absorption spectroscopy (XAS) and electron energy loss spectroscopy (EELS).[7−10] Further, we explain the origin of the line splitting from fundamental concepts described in the Hückel and Clar models of MOs in PAHs.

METHODS

Carbon K-edge XRS probes transitions between 1s electrons and higher-lying σ^* and π^* unoccupied MOs. In the dipole limit (i.e., low momentum transfer), XRS spectra are formally equivalent to conventional soft X-ray absorption spectra (XAS), except XRS probes the bulk sample, while XAS is rather surface sensitive.[11−13] The bulk sensitivity makes XRS attractive for analysis of complex mixtures and samples prone to oxidation, where the surface may not be representative of the bulk. Here we report spectra acquired with a high-resolution XRS spectrometer operated at beamline 6-2 at the Stanford Synchrotron Radiation Laboratory.[14] Briefly, the instrument consists of 40 crystal Si(440) analyzers arranged on overlapping Rowland circles of 1000 mm and at a fixed Bragg angle of 88° resulting in a fixed detection energy at 6462.0 eV and an energy resolution of 0.29 eV. Through a Si(311)

Received: May 23, 2018
Revised: June 6, 2018
Published: June 13, 2018

DOI: 10.1021/acs.jpca.8b04922
J. Phys. Chem. A 2018, 122, 5730−5734

double-crystal monochromator, carbon 1s XRS spectra are recorded with the inverse scanning methodology, i.e. while the detection energy is kept fixed at 6462.2 eV, the incident energy is scanned across the range of 6732.2−6767.2 eV to capture an energy transfer range of 270 to 305 eV. The average momentum transfer captured from the extended 40 crystal spectrometer, when accounting the $\sin^2(\theta/2)$ dependence of the XRS signal, is $q \sim 1.23$ au, which ensures that the dipole transitions dominate the XRS spectrum.[13] Additionally, these electronic transitions were calculated using an excited state Hückel method coupled with excited state density functional theory (DFT). Briefly, the relative energy of the lowest unoccupied molecular orbitals (LUMOs) are calculated by modeling the excited carbon atom as a nitrogen atom.[15] To place the molecular orbital energies on an absolute scale, the orbital energies were subtracted from the average ionization energy for a carbon atom in these molecules (∼291 eV). The average ionization energy and the dipole transition intensity were calculated using excited state density functional theory (DFT) using the StoBe package.[16] All calculations were performed for the ground state molecules and excited state for each symmetrically unique core hole. All molecular orbital diagrams were prepared by taking a linear combination of hydrogenic p_z orbitals with the coefficients obtained by following Huckel's method.

RESULTS AND DISCUSSION

As described by the Clar model, π bonds in PAHs are divided into aromatic sextets (AS) and isolated double bonds (IDB).[5] AS contain π electrons that are fully delocalized over the carbon hexagon. They are the most aromatic centers in PAHs and indicate regions of local aromaticity in large molecules.[17,18] Consistent with the stability of aromatic rings resulting from electron delocalization, AS contribute to the kinetic stability of PAHs by increasing the HOMO−LUMO gap.[19] IDB, on the other hand, have polyene-like character and can be as reactive as olefinic double bonds in unconjugated molecules.[5,18,20] The most probable electronic structure of a PAH is one in which the number of AS is maximized while the number of IDB is minimized, and algorithms such as the Y-rule have been developed to identify these electronic structures.[18,20−22]

Figure 1 presents the XRS spectra of several PAHs in the region near 285 eV, which probes the core level excitations from carbon 1s orbitals into the lowest unoccupied molecular orbitals of π character, denoted 1s−π^* transitions.[23] PAHs are presented in order of increasing fraction of the π bonds that are IDB. The electronic structures of the PAHs as described by the Clar model are drawn, with AS indicated by an inscribed circle as in benzene, and IDB indicated by an explicit double bond as in an olefin (resonant structures with the same % IDB are equally probably but are not shown). A peak splitting is observed in the spectra, and the magnitude of that splitting increases with the % IDB. The spectrum of triphenylene (0% IDB) appears as a singlet or very closely spaced doublet, similar to the spectrum of other fully benzenoid PAHs such as graphite.[14,24] The magnitude of the splitting increases up to 2 eV for pentacene (73% IDB), the highest %IDB PAH studied here.

These results are consistent with previously reported core electron spectra of PAHs. Bergmann et al.,[6] working with a lower-resolution XRS spectrometer, observed a line broadening that increased with %IDB in the spectra of a limited set PAHs. Splittings similar to those observed here were obtained

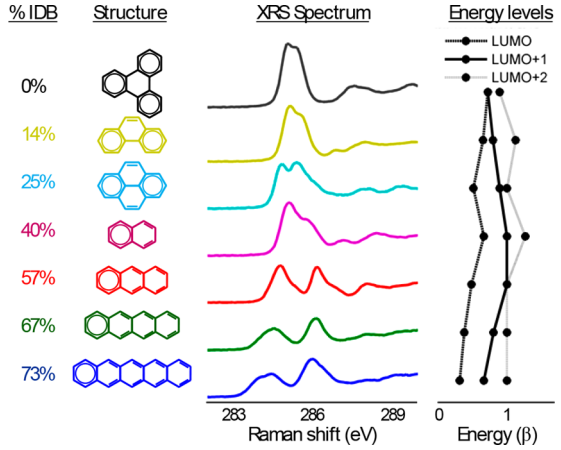

Figure 1. Fraction of π bonds that are IDB (first column); Clar structure (second column); measured 1s−π^* XRS spectrum (third column); and energies of the first three unoccupied energy levels (fourth column) for a series of PAHs. The energy scale is in units of the energy of the resonance integral β. The PAHs presented are triphenylene, phenanthrene, pyrene, naphthalene, anthracene, tetracene, and pentacene (top to bottom).

in earlier measured and calculated XAS spectra of anthracene (57% IDB),[25] nondeuterated and perdeuterated pyridine,[26] a series of linearly concatenated PAHs (polyacenes)[8] and smaller PAH subsets,[7] nondeuterated and perdeuterated naphthalene (40% IDB),[27] and various medium sized PAHs,[9,10] each studied separately.

However, the mechanisms proposed to explain those observations (which were applied to only a small number of PAHs) do not provide a satisfactory explanation of the present results (which encompass a broad set of PAHs), as described below. While the line broadening observed in PAHs was previously successfully employed to assess the structure of complex mixtures, a physical mechanism explaining the origin of the broadening was not provided.[6] The spectrum of anthracene was calculated precisely when including relaxation effects caused by excitations from localized core hole states, but calculations of other PAHs were not performed, so trends across PAHs were not considered.[25] The splitting in nondeuterated and perdeuterated pyridine was attributed to chemical shift differences based on the position of the carbon atoms relative to the nitrogen atom, but that effect does not apply to the unsubstituted PAHs studied here.[26] Chemical shift differences between different carbons in polyacenes were shown to contribute to the splitting[8] and were invoked as a potentially significant effect in the spectra of smaller PAH subsets.[7] However, as noted earlier,[25] variations due to chemical shift are too small (typically <0.5 eV) to be responsible for the majority of the observed splitting presented in Figure 1. Studies of deuterated molecules demonstrated that vibrational fine structure is responsible for relatively small splittings in the core electron spectra of PAHs,[26,27] but vibrational structure cannot be the main cause of the larger splittings observed here, which extend up to an order of magnitude larger than the relevant vibrational energies. Gordon et al.[7] studied a subset of smaller PAHs in great detail using a local Gaussian based DFT method. Although close agreement between theory and experiment was obtained, a simplified interpretation of the findings that rationalizes the observed energetics is difficult to extract. Among other findings, these results generated a hypothesis that the line

DOI: 10.1021/acs.jpca.8b04922
J. Phys. Chem. A 2018, 122, 5730−5734

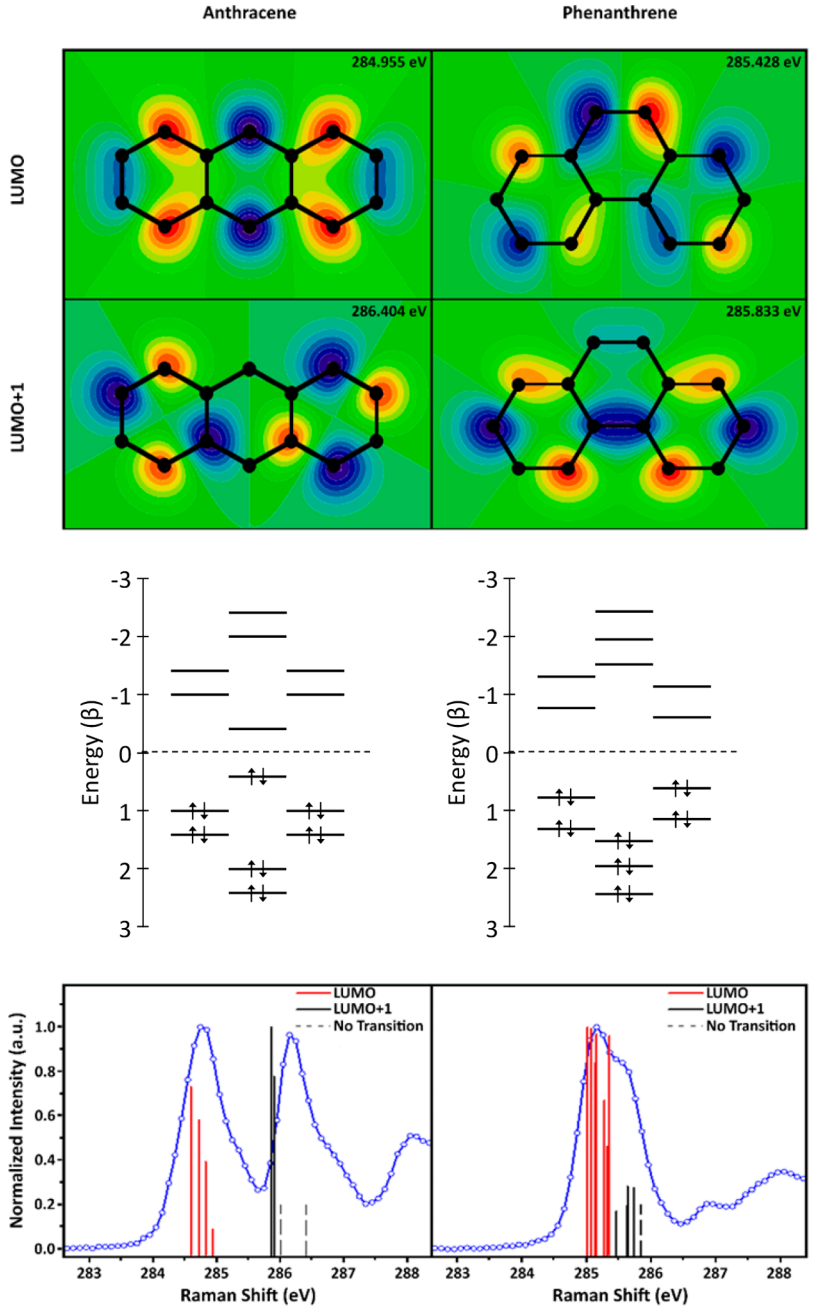

Figure 2. Molecular orbitals and XRS transitions for anthracene (left) and phenanthrene (right). Top panels show ground state wave function contour maps (red and blue indicate maximum amplitude of opposite phase, green indicates zero amplitude) of the LUMO and LUMO+1, illustrating nodes on several carbon nuclei; middle panel shows the energy levels of the π and π^* orbitals, illustrating a relative increase of the HOMO and decrease of the LUMO−LUMO+1 gap in phenanthrene; bottom panel shows simulated transition energies and intensities (including core hole effects) from core electrons bound to each inequivalent carbon along with the measured spectrum, illustrating the varying energetics and transition amplitudes from the different unique carbons into the LUMO and the LUMO+1. Transitions drawn with dotted lines have a transition probability of 0 and correspond to carbon atoms on nodes in the molecular orbitals.

broadening is related to symmetry, with molecules containing a greater number of inequivalent carbons yielding a broader line (the authors cautioned that insufficient data were available to reach a firm conclusion).[7] That hypothesis is inconsistent with these high-resolution data showing that phenanthrene (14% IDB, 7 inequivalent carbons) has a narrower splitting than anthracene (57% IDB, 4 inequivalent carbons).

Here we show that the origin of the splitting of the 1s−π^* transition in PAHs can primarily be explained using Hückel theory based on ground state energetics. This model does not perfectly reproduce the experimental spectra, but the objective here is to provide a simple conceptual picture that captures the dominant effects. This model neglects effects such as the influence of the core hole, which results in some deviations that will be addressed in separate studies. However, this approximation does not significantly impact the general trends (see SI), consistent with prior calculations showing the distortion of low-lying MOs due to the core hole is modest in large PAHs.[9,10,25] For simplicity, the model is described here using phenanthrene (14% IDB) and anthracene (57% IDB) as

DOI: 10.1021/acs.jpca.8b04922
J. Phys. Chem. A 2018, 122, 5730−5734

examples. These two molecules are chosen as examples, because they differ widely in the extent of spectral splitting despite being structurally similar $C_{14}H_{10}$ isomers.

The measured carbon XRS spectra in this energy range comprise the sum of signals resulting from electronic transitions originating from 1s orbitals on each of the carbons and going to each of multiple unoccupied MOs. The unoccupied MOs probed in this energy range for all carbon sites are the lowest unoccupied molecular orbital (LUMO) and the next few lowest orbitals (LUMO+1, LUMO+2, etc.), all of which have mostly π^* character. The transition intensity depends on the geometry of both the initial and final state wave functions, according to Fermi's Golden Rule in the dipole approximation. Because the 1s wave function decays exponentially with distance, the transition intensity is nearly proportional to the amplitude of the unoccupied MO at the excited carbon nucleus. The π^* orbitals have several nodes (successively higher-energy MOs contain additional nodes, and the lowest energy MOs are occupied), and in most cases, several nodes occur near carbon nuclei. For example, Figure 2 presents calculated LUMOs for anthracene and phenanthrene, illustrating LUMO nodes located near four and two carbon nuclei and LUMO+1 nodes located near six and two carbon nuclei (respectively). Because of these nodes, transitions originating on some carbons go primarily to the LUMO, while transitions originating on other carbons go primarily to the LUMO+1 or other MOs. The experimental spectrum represents the sum of all of these transitions.

The transition energies are essentially independent of which carbon binds the excited core electron, because 1s orbitals belonging to different carbon nuclei in PAHs have essentially the same energy. However, the transition energy depends on the MO to which the core electron is moved, with higher-lying MOs resulting in transitions at higher energies. For PAHs, the energies of those orbitals are given by the Clar and Hückel models.[5,19] Relative to MOs associated with IDB, MOs associated with AS are characterized by wide HOMO−LUMO gaps (which contributes to their stability).[19] Thus, the HOMO−LUMO gaps of PAHs increase with the %AS. Because the MO energies are distributed symmetrically relative to the energy of the uncombined 2p orbitals, molecules with wide HOMO−LUMO gaps have relatively high-lying LUMOs (and low-lying HOMOs). However, the energies of the higher-lying LUMO+1 and LUMO+2 are nearly independent of whether the PAH is dominated by AS or IDB. As a result, when the LUMO energy is increased (as occurs in PAHs rich in AS), the LUMO will be close in energy to the LUMO+1 and perhaps the LUMO+2; while when the LUMO energy is decreased (as occurs in PAHs rich in IDB), the LUMO will be far in energy from the LUMO+1 and LUMO+2. This effect can be see for phenanthrene and anthracene in the middle panel of Figure 2, which plots the energies of all occupied and unoccupied π orbitals as estimated by the simple Hückel theory. In the Hückel theory, the MO energies relative to the energies of the uncombined 2p orbitals are expressed in terms of the energy of the resonance integral β, typically around −2 eV (if calculated from ionization energies). Phenanthrene is rich in AS (14% IDB), has a relatively high-lying LUMO ($0.605|\beta|$), and a small gap between the LUMO and the LUMO+1 ($0.164|\beta|$); meanwhile anthracene is rich in IDB (57% IDB), has a relatively low-lying LUMO ($0.414|\beta|$), and a large gap between the LUMO and the LUMO+1 ($0.586|\beta|$).

The difference in those orbital energies is then responsible for the observed splitting: for PAHs with low %IDB, the LUMO is pushed up, becoming nearly degenerate with the LUMO+1 and LUMO+2, such that transitions to any of these π^* MOs occur at nearly the same energy and appear as a singlet or very closely spaced doublet in the measured spectra. For PAHs with high %IDB, the LUMO is lowered, creating a large gap to the LUMO+1 and LUMO+2, such that transitions to the different π^* MOs occur at distinct energies and appear as a split line in the measured spectra. The bottom panel of Figure 2 shows this effect for phenanthrene and anthracene. The calculated energy and intensity of transitions from each inequivalent carbon to both the LUMO and the LUMO+1 are shown explicitly for both molecules. The measured spectra are also shown and comprise the sum of all these transitions. Transitions from certain initial carbon 1s orbitals to certain π^* orbitals are considerably more intense than others (including some transitions with near zero intensity) because of the π^* nodes discussed earlier. Transitions from the different initial carbon 1s orbitals to the same π^* orbital vary in energy over a limited range because of the limited chemical shift effects also discussed earlier. Instead, the spectra are dominated by the differences in energy between transitions terminating on the LUMO and transitions terminating on the LUMO+1. In phenanthrene, those transitions are sufficiently close in energy to be essentially unresolved, resulting in the measured singlet; while in anthracene, those transitions are widely separated, resulting in the measured doublet. The close agreement between measured spectra and calculated energy levels validates the explanation proposed here, unlike previous models, which cannot explain splittings as large as experimentally observed.

CONCLUSION

The measured trend of splitting in the 1s−π^* transitions in some PAHs but not in others is explained in terms of the Clar and Hückel models of aromaticity. This simple model considering only ground state energetics is shown to capture the majority of the physics, although more sophisticated models are required to reproduce the measured spectra exactly. According to the Clar model, PAHs of different geometries contain different amounts of AS (which are associated with relatively high-lying LUMOs) versus IDB (which are associated with relatively low-lying LUMOs). Hückel calculations of the energies of the LUMO, LUMO+1, and LUMO+2 of various PAHs show that high-lying LUMOs cause small LUMO−LUMO+1 gaps, while low-lying LUMOs cause large LUMO−LUMO+1 gaps. Thus, PAHs rich in AS have nearly degenerate π^* orbitals leading to a nearly singlet 1s−π^* transition, while PAHs rich in IDB have widely separated π^* orbitals leading to a split 1s−π^* transition. This result can be seen in the final column of Figure 1, which plots the energies of the LUMO, LUMO+1, and LUMO+2 relative to the energy of the uncombined 2p orbitals. For PAHs with low %IDB, these three orbitals are nearly degenerate, and a singlet or very closely spaced doublet is observed in the spectra. As the %IDB increases, the orbital energies become more widely spaced and a spectral splitting is observed.

ASSOCIATED CONTENT

Supporting Information

The Supporting Information is available free of charge on the ACS Publications website at DOI: 10.1021/acs.jpca.8b04922.

DOI: 10.1021/acs.jpca.8b04922
J. Phys. Chem. A 2018, 122, 5730−5734

Details of the experimental procedure, details of the calculations, sensitivity to the core hole, comparison of LUMO and LUMO+1 energy difference for all PAH's in Figure 1 (PDF)

AUTHOR INFORMATION

Corresponding Author

*E-mail: apomerantz@slb.com.

ORCID

Andrew E. Pomerantz: 0000-0003-2639-2682

Notes

The authors declare no competing financial interest.

ACKNOWLEDGMENTS

Use of the Stanford Synchrotron Radiation Lightsource, SLAC National Accelerator Laboratory, is supported by the U.S. Department of Energy, Office of Science, Office of Basic Energy Sciences under Contract No. DE-AC02-76SF00515.

REFERENCES

(1) Kekulé, A. Sur la constitution des substances aromatiques. *Bull. Soc. Chim. Fr.* **1865**, *3*, 98−110.

(2) Hückel, E. Quantentheoretische Beiträge zum Benzolproblem II. *Eur. Phys. J. A* **1931**, *72*, 310−337.

(3) Hückel, E. Quantentheoretische Beiträge zum Benzolproblem. *Eur. Phys. J. A* **1931**, *70*, 204−286.

(4) Hückel, E. Quantentheoretische Beiträge zum Problem der aromatischen und ungesättigten Verbindungen. III. *Eur. Phys. J. A* **1932**, *76*, 628−648.

(5) Clar, E. *The Aromatic Sextet*; John Wiley & Sons: London, 1972.

(6) Bergmann, U.; Groenzin, H.; Mullins, O. C.; Glatzel, P.; Fetzer, J.; Cramer, S. P. Carbon K-edge X-ray Raman spectroscopy supports simple, yet powerful description of aromatic hydrocarbons and asphaltenes. *Chem. Phys. Lett.* **2003**, *369*, 184−191.

(7) Gordon, M. L.; Tulumello, D.; Cooper, G.; Hitchcock, A. P.; Glatzel, P.; Mullins, O. C.; Cramer, S. P.; Bergmann, U. Inner-Shell Excitation Spectroscopy of Fused-Ring Aromatic Molecules by Electron Energy Loss and X-ray Raman Techniques. *J. Phys. Chem. A* **2003**, *107*, 8512−8520.

(8) Ågren, H.; Vahtras, O.; Carravetta, V. Near-edge core photoabsorption in polyacenes: model molecules for graphite. *Chem. Phys.* **1995**, *196*, 47−58.

(9) Yokoyama, T.; Seki, K.; Morisada, I.; Edamatsu, K.; Ohta, T. X-Ray Absorption Spectra of Poly-*p*-Phenylenes and Polyacenes: Localization of π^* Orbitals. *Phys. Scr.* **1990**, *41*, 189−192.

(10) Oji, H.; Mitsumoto, R.; Ito, E.; Ishii, H.; Ouchi, Y.; Seki, K.; Yokoyama, T.; Ohta, T.; Kosugi, N. Core hole effect in NEXAFS spectroscopy of polycyclic aromatic hydrocarbons: Benzene, chrysene, perylene, and coronene. *J. Chem. Phys.* **1998**, *109*, 10409.

(11) Bergmann, U.; Glatzel, P.; Cramer, S. P. Bulk-sensitive XAS characterization of light elements: from X-ray Raman scattering to X-ray Raman spectroscopy. *Microchem. J.* **2002**, *71*, 221−230.

(12) Mizuno, Y.; Ohmura, Y. Theory of X-Ray Raman Scattering. *J. Phys. Soc. Jpn.* **1967**, *22*, 445−449.

(13) Schülke, W. *Electron Dynamics by Inelastic X-Ray Scattering*; Oxford Series on Synchrotron Radiation; Oxford University Press, 2007.

(14) Sokaras, D.; Nordlund, D.; Weng, T. C.; Mori, R. A.; Velikov, P.; Wenger, D.; Garachtchenko, A.; George, M.; Borzenets, V.; Johnson, B.; Qian, Q.; Rabedeau, T.; Bergmann, U. A high resolution and large solid angle x-ray Raman spectroscopy end-station at the Stanford Synchrotron Radiation Lightsource. *Rev. Sci. Instrum.* **2012**, *83*, 043112.

(15) Hoffmann, R. Extended Hückel Theory. III. Compounds of Boron and Nitrogen. *J. Chem. Phys.* **1964**, *40*, 2474−2480.

(16) Hermann, K.; Pettersson, L. G. M.; Casida, M. E.; Daul, C.; Goursot, A.; Koester, A.; Proynov, E.; St-Amant, A.; Salahub, D. R.; et al. *StoBe-deMon*, version 3.3; 2014.

(17) Portella, G.; Poater, J.; Solà, M. Assessment of Clar's aromatic π-sextet rule by means of PDI, NICS and HOMA indicators of local aromaticity. *J. Phys. Org. Chem.* **2005**, *18*, 785−791.

(18) Vijayalakshmi, K. P.; Suresh, C. H. Pictorial representation and validation of Clar's aromatic sextet theory using molecular electrostatic potentials. *New J. Chem.* **2010**, *34*, 2132.

(19) Aihara, J.-i. Reduced HOMO-LUMO Gap as an Index of Kinetic Stability for Polycyclic Aromatic Hydrocarbons. *J. Phys. Chem. A* **1999**, *103*, 7487−7495.

(20) Ruiz-Morales, Y. The Agreement between Clar Structures and Nucleus-Independent Chemical Shift Values in Pericondensed Benzenoid Polycyclic Aromatic Hydrocarbons: An Application of the Y-Rule. *J. Phys. Chem. A* **2004**, *108*, 10873−10896.

(21) Ona-Ruales, J. O.; Ruiz-Morales, Y. Extended Y-rule method for the characterization of the aromatic sextets in cata-condensed polycyclic aromatic hydrocarbons. *J. Phys. Chem. A* **2014**, *118*, 12262−73.

(22) Randić, M. Aromaticity of Polycyclic Conjugated Hydrocarbons. *Chem. Rev.* **2003**, *103*, 3449−3606.

(23) Stöhr, J. *NEXAFS Spectroscopy*; Springer Series in Surface Sciences; Springer: Berlin, 1992; p 403.

(24) Bergmann, U.; Mullins, O. C.; Cramer, S. P. X-ray Raman Spectroscopy of Carbon in Asphaltene: Light Element Characterization with Bulk Sensitivity. *Anal. Chem.* **2000**, *72*, 2609−2612.

(25) Klues, M.; Hermann, K.; Witte, G. Analysis of the near-edge X-ray-absorption fine-structure of anthracene: a combined theoretical and experimental study. *J. Chem. Phys.* **2014**, *140*, 014302.

(26) Kolczewski, C.; Püttner, R.; Plashkevych, O.; Ågren, H.; Staemmler, V.; Martins, M.; Snell, G.; Schlachter, A. S.; Sant'Anna, M.; Kaindl, G.; Pettersson, L. G. M. Detailed study of pyridine at the C 1s and N 1s ionization thresholds: The influence of the vibrational fine structure. *J. Chem. Phys.* **2001**, *115*, 6426.

(27) Hübner, D.; Holch, F.; Rocco, M. L. M.; Prince, K. C.; Stranges, S.; Schöll, A.; Umbach, E.; Fink, R. Isotope effects in high-resolution NEXAFS spectra of naphthalene. *Chem. Phys. Lett.* **2005**, *415*, 188−192.

DOI: 10.1021/acs.jpca.8b04922
J. Phys. Chem. A 2018, 122, 5730−5734